An Improved Approach to the Predictability & Reliability of the Onset of Turbulence with Shocks

***H.C. Yee*[1] *and Björn Sjögreen*[2]**
[1] ***MS 258-5, NASA Ames Research Center, Moffett Field, CA, USA***
[2] ***Multid Analyses AB, Sweden***
Helen.M.Yee@nasa.gov

Abstract

The construction of numerical schemes for (a) stable and accurate simulation of turbulence with strong shocks, and for (b) obtaining correct propagation speed of discontinuities in the presence of stiff source terms share one important ingredient – minimization of numerical dissipation while maintaining numerical stability. The dual requirements to achieve both numerical stability and minimal numerical dissipation are often conflicting since existing shock capturing schemes were designed mainly to be robust for rapidly developed turbulence-free flows and for shock waves without stiff source term. For the past two decades, Yee and collaborators have focused on an improved understanding of the nonlinear behavior of different high order shock-capturing methods. It was found that even very high order methods without proper nonlinear stability and numerical dissipation control can either numerically smear the onset of turbulence due to excess numerical dissipation, or induce (onset) numerical turbulence that is not physical turbulence due to lack of proper numerical dissipation to improve nonlinear stability for long time integration. Our approach is to combine (I) and (II) below for obtaining the physically correct onset of turbulence with shocks, including problems with stiff source terms:
(I) Nonlinear dynamics is utilized to complement the traditional linearized stability theory (Yee & Sweby, Yee et al., Griffiths et al., Lafon & Yee, Yee, Wang et al., Kotov et al. 1990- 2015) in order to (i) Minimize numerically induced false transition to turbulence, (ii) Minimize numerical instability due to long time integration of turbulent flows, (iii) Minimize numerically induced standing wave solutions, and (iv) Minimize wrong propagation of speed of discontinuities due to the presence of stiff source terms.
(II) Our recently developed physical preserving (structural preserving) high order methods with improved nonlinear stability & accuracy that are essential in minimizing spurious numerics are used.

1 Motivation

Our motivation is to ensure a higher level of confidence in the predictability and reliability of numerical simulation for multiscale complex nonlinear fluid problems. The last two decades have been an era when computation is ahead of analysis and when very large scale practical computations are increasingly used in poorly understood multiscale complex nonlinear physical problems and non-traditional fields, especially when computations offer the *only* way of generating this type of data limited simulations. At present some of the numerical uncertainties can be explained and minimized by traditional numerical analysis and standard CFD practices, complementing with experimental data. However, such practices, usually based on linearized analysis, *might not* be sufficient for strongly nonlinear and/or stiff problems. We need a good understanding of the nonlinear behavior of numerical schemes being used as an integral part of code verification, validation and certification. Unlike linear model equations used for conventional stability and accuracy considerations in time-dependent partial differential equations (PDEs), there are no equivalent unique nonlinear model equations for nonlinear hyperbolic and parabolic PDEs for fluid dynamics. On the one hand, a numerical method behaving in a certain way for a particular nonlinear PDE might exhibit a different behavior for a different nonlinear PDE even though the PDEs are of the same type. On the other hand, even for simple nonlinear model PDEs with known solutions, the discretized counterparts can be extremely complex, depending on the numerical methods, their time steps, grid spacings and numerical boundary condition treatments. Except in special cases, there is no general theory at the present time to characterize the various nonlinear behaviors of the underlying discretized counterparts.

In addition, it is common knowledge by the numerical simulation of turbulent flow community that even modern high order shock-capturing methods, that were designed for rapidly developing flows, are too dissipative for turbulent flow computations. The basic ingredients that are needed for efficient accurate and reliable simulation of the subject flow are: (a) Numerically preserving as much of the physical properties of the flows (e.g., positive pressure and density; preservation of the divergence of the magnetic field, if present; entropy conserving; momentum conserving and kinetic energy preserving), (b) Correct numerically handling of stiff source terms, if present, (c) Improved numerical stability but at the same time minimization of added numerical dissipation for long time integration of flows containing both the shock-free turbulence regions and turbulence with shocks regions. The new high order methods developed by our work contain most of these desirable properties as well as they are most suited and efficient for high performance implementation for current modern supercomputers.

The work leverages our knowledge gained in (1) Nonlinear behavior of numerical methods to complement the traditional linearized stability theory (Yee & Sweby, Yee et al., Griffiths et al., Lafon & Yee, Yee, Wang et al., Kotov et al. 1990- 2015), and (2) our new physical-preserving (structure-preserving) high order numerical methods in conjunction with our high order nonlinear filter methods of Yee & Sjögreen, Sjögreen & Yee for compressible shock-turbulence interaction with improved nonlinear stability and accuracy. The high order nonlinear filter methods of Yee & Sjögreen, Sjögreen & Yee and collaborators represent the culmination of over 20 years of development. They have been successfully used to simulate numerous examples of flows containing turbulence and shocks. These physical preserving methods can improve nonlinear stability and minimize aliasing error for turbulence modeling and simulation; see [13, 15, 16, 30, 31]. In addition, for the last decade it has been shown in the literature that these high order methods are able to reduce the amount of added numerical dissipation required to avoid nonlinear instabilities from developing in direct numerical simulations (DNS) computations.

2 Insufficient Numerical Dissipation Without Nonlinear Stability Control Can Induce Numerical On Set of Turbulence that is Not Physical Turbulence

For detailed discussion, see Yee (2002) [22] and references cited therein. Fig. 6.2 of Sections 6.3-6.3 in [22] gives a summary of different scenarios of possible numerical bifurcation of transition to turbulence (false transition of a studied Reynold's number) for a chosen spatial and temporal discretization as a function of the grid spacing and time step parameters. Fig. 6.2 of [22] is included below.

Chaotic and Chaotic Transient In addition to the inherent chaotic and chaotic transient behavior in some physical systems, numerics can independently introduce numerical chaos, numerical chaotic transients, as well as suppress physical chaos. Loosely speaking, a chaotic transient behaves like a chaotic solution. A chaotic transient can occur in a continuum or a discrete dynamical system indicating turbulence-like behavior. Using highly accurate methods for rapidly developed flows for long time integration of turbulent flows, nonlinear instability can occur that resembles chaotic-like numerical turbulence, in-distinguishable from physical turbulence. Moreover, one of the major characteristics of a numerically induced chaotic transient is that if one does not integrate the discretized equations long enough, the numerical solution has all the characteristics of a chaotic solution. The required number of time integration steps might be far beyond those found in standard CFD simulation practice before the numerical solution can get out of the chaotic transient mode. Furthermore, standard numerical methods, depending on the initial data, usually experience drastic reductions in step size and convergence rate near a bifurcation point (e.g., transition point) of the continuum in addition to the bifurcation points due solely to the discretized parameters. See Yee et al., Yee & Sweby (1990-2013) for a discussion and some numerical results. Consequently, a possible numerically induced chaotic transient is especially worrisome in direct numerical simulations (DNS) of the transition from laminar to turbulent flows. Except for special situations, it is extremely difficult to bracket closely the physical transition point by mere DNS of the Navier-Stokes equations. Even away from the transition point, this type of numerical simulation is already very CPU intensive and the convergence rate is usually rather slow. Due to limited computer resources, the numerical simulation can result in chaotic transients indistinguishable from sustained turbulence, yielding a spurious picture of the flow for a given Reynolds number. Consequently, it casts some doubt on the reliability of numerically predicted transition points and chaotic flows. It also influences the true connection between chaos and turbulence. It is noted that due to excessive numerical dissipation, some numerics can suppress physical turbulence.

Numerical Transition Aside from illustrating numerical examples on the possible numerical chaotic transients that are indistinguishable from sustained turbulence, Yee and collaborators [22] illustrated many examples of the onset of numerical turbulence as a function of the chosen numerical method, time step and grid spacing. Assuming a known physical bifurcation or transition point, Fig. 6.2 from [22] illustrates the schematic of four possible spurious bifurcations due to constant time steps and constant grid spacings.

3 Wrong Propagation of Discontinuity due to Stiff Nonlinear Source Terms

Here an unsteady non-equilibrium inviscid computation from [28, 6] is chosen as an illustration. Navier-Stokes computations of the same test case in 1D and 2D can be found in [6]. For combustion and random forcing terms, see [24, 28, 6, 7] and references cited therein. In general, the reacting terms that arise from non-equilibrium flows in hypersonic aeronautics are less stiff than their counterparts in combustion. However, there are stiff chemical non-equilibrium flows

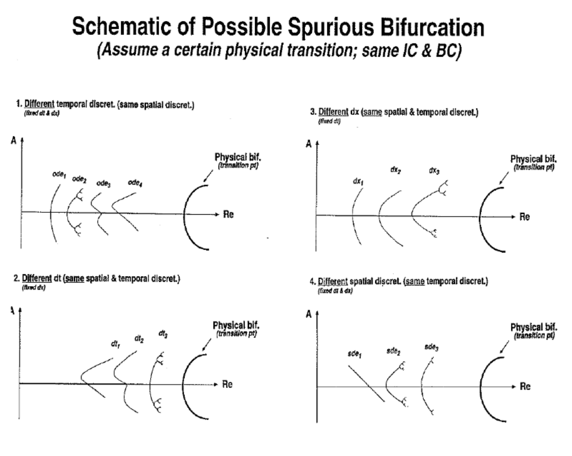

Figure 6.2. *Schematic of possible spurious bifurcation for constant time steps and grid spacings. (1) Different temporal discretizations ode_1, ode_2, ode_3 and ode_4 (same spatial discretization and the same constant dt and dx). (2) Different constant time steps dt_1, dt_2, dt_3 and dt_4 (same temporal and spatial discretizations, and the same constant dx). (3) Different constant grid spacings dx_1, dx_2, dx_3 and dx_4 (same spatial and temporal discretizations, and the same constant dt). (4) Different spatial discretizations sde_1, sde_2 and sde_3 (same temporal discretization and the same constant dt).*

that are due to the reaction terms. A stiff 13-species, one-temperature non-equilibrium model related to the NASA Ames Electric Arc Shock Tube (EAST) experiment reported in [28, 6] is briefly illustrated here for the 1D case. See [28, 6] for extensive analysis and a wide variety of other spurious numerics illustrations due to presence of shock waves and stiff source terms. The computational domain of the 1D 13-species EAST test case has a total length of $8.5m$. The left part of the domain with length $0.1m$ is a high pressure region. The right part of the domain with length $8.4m$ is a low pressure region. The gas mixture consists of 13 species:

$$e^-, He, N, O, N_2, NO, O_2, N_2^+, \\ NO^+, N^+, O_2^+, O^+, He^+.$$

See [28, 6] for initial conditions and problem set up.

Although figures not shown, grid refinement for four grids with $\Delta x = 10^{-3}\ m$, $5 \times 10^{-4}\ m$, $5 \times 10^{-5}\ m$ and $2.5 \times 10^{-5}\ m$ at time $t_{end} = 0.325 \times 10^{-4}\ sec$ indicated a significant shift in the shear (left discontinuity) and the shock (right discontinuity) locations as the grid is refined. The distance between the shear and the shock shrinks as the grid is refined. The difference between shock locations obtained on the grids with $\Delta x = 5 \times 10^{-5}\ m$ and $2.5 \times 10^{-5}\ m$ is less than 0.3%. Thus the solution using $\Delta x = 5 \times 10^{-5}\ m$ can be considered as the reference solution.

Taking Fig. 2 from [28], the left subfigure shows a comparison among five methods obtained on a coarse grid ($\Delta x = 10^{-3}\ m$) with the reference solution. The scheme's labels are defined as follows:

- ACMTVDfi: Second-order central base scheme using ACM flow sensor. See [20] for further information on filter schemes.

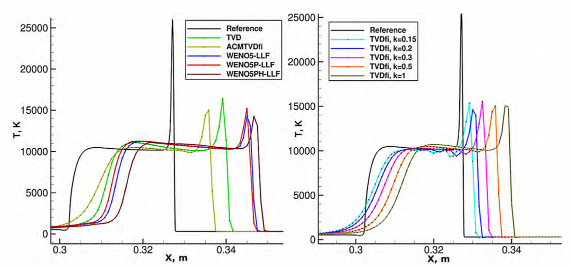

Fig. 2. 1D, 13 species EAST problem: comparison among methods using 601 point grids with $CFL = 0.6$ and $t_{end} = 3.25 \times 10^{-5}$ s. Left subfigure: Reference solution (TVD on a 10,001 point grid) (line 1), TVD (line 2), ACMTVDfi (TVDfi) using $\kappa = 0.5$ (line 3), WENO5-llf (line 4), WENO5P-llf (line 5), WENOPH-llf (line 6). Right: ACMTVDfi, $\kappa = 0.15$ (line 2), $\kappa = 0.2$ (line 3), $\kappa = 0.3$ (line 4), $\kappa = 0.5$ (line 5), $\kappa = 1$ (line 6). See text for method notation.

- WENO5-llf: Fifth-order WENO (WENO5) using the local Lax-Friedrichs flux.
- WENO5P-llf: Positive WENO5 of using the local Lax-Friedrichs flux.
- WENO5PH-llf: Positive WENO5 of using the local Lax-Friedrichs flux.

The right subfigure shows a comparison of ACMTVDfi using a different weight κ parameter of the ACM flow sensor. The smaller the κ, the smaller the amount of TVD dissipation used. Among the considered schemes, the result indicates that the least dissipative scheme predicts the shear and shock locations best when compared with the reference solution. The results indicate that ACMTVDfi is slightly more accurate than WENO5-llf. This is due to the fact that ACMTVDfi reduces the amount of numerical dissipation away from high gradient regions. Using the subcell resolution method of [24] for one reaction case by applying it to only one of the reactions in this multi-reaction flow does not improve the performance over standard schemes. Further research on the generalization of subcell resolution to multi-reactions needs to be explored.

4 Numerical Dissipation Control and Structure-Preserving High Order Methods

Newer turbulence/shock simulations use adaptive blending of variant of high order ENO/WENO shock-capturing methods and high order non-dissipative methods in such a way that high order WENO schemes are active only near the shock wave, and the methods free from numerical dissipation are used in the turbulent flow away from the shock. There are basically two camps of such development: (a) The hybrid method that switches between high order non-dissipative methods and high order shock-capturing methods (e.g., high order WENO or ENO), and (b) High order nonlinear filter method of Yee et al., Sjögreen & Yee, Yee & Sjögreen and Kotov et al. [20, 10, 25, 27, 12, 29, 30, 13, 15, 16, 30, 31]. These two general approaches, if with proper control of the amount of numerical dissipation, usually provide a similar accuracy. However, the nonlinear filter approach is more efficient.

The nonlinear filter methods are efficient in suppressing spurious oscillations at discontinuities and high-frequency oscillations in systems of strongly coupled nonlinear equations. The idea was first introduced and tested by Yee et al. [20], using an artificial compression method (ACM) of Harten as the flow sensor. Later, multiresolution wavelet and other smart flow sensors were developed by Sjögreen & Yee, Yee & Sjögreen, and Kotov et al. [27, 7]. The smart sensor flags the locations, estimates the amount of numerical dissipation needed at these locations, and keeps the rest of the flow field free of shock-capturing dissipation. The nonlinear filter schemes are efficient. The total computational cost for a given error tolerance is significantly lower than for standard shock-capturing schemes or their hybrid cousins of the same order. One important reason for their efficiency is that the nonlinear shock-capturing filter dissipation is applied after each full time step, whereas a standard shock-capturing/hybrid method evaluates the shock-capturing dissipation at each stage of the, e.g, Runge-Kutta (R-K) time stepping scheme. Hence, the nonlinear filter approach requires only one Riemann solve per time step per grid point per dimension, independent of the time discretization involved. Hybrid schemes, which switch between high order non-dissipative methods and high order shock-capturing method within the same R-K stage, are less efficient than the nonlinear filter methods.

All of the recently developed high order nonlinear filter methods that use base schemes (i.e., discretizations before applying the filter) that are entropy conserving, momentum conserving, kinetic energy preserving or combine two or more of these physical property preserving discretizations are already included in our 3D ADPDIS3D computer code developed by Sjögreen & Yee. The code has been used to simulate benchmark problems for turbulence with shocks in gas dynamics [4, 27, 26], and for solving the equations of MHD [23, 29, 30, 13, 15, 16, 30, 31].

An Illustration of the performance of structure-preserving high order nonlinear filter method

The methods for comparison in this paper for spatial discretizations are:

- ECHKP: Entropy conserving using the Harten class of entropy functions $E_H = -\frac{\gamma+\alpha}{\gamma-1}\rho(p\rho^{-\gamma})^{\frac{1}{\alpha+\gamma}}$ [18, 3]. It turned out that this method in its base form also satisfies Ranocha's kinetic energy preservation condition (KEP); so there is only one variant for this method [11, 9].

- ECLOG: Tadmor-type entropy conserving method using the entropy function $E_L = -\rho\log(p\rho^{-\gamma})$.

- ES: Skew-symmetric splitting of the inviscid flux derivative that is entropy conserving and stable using the Harten entropy function [3] and the generalized energy norm with summation-by-parts (SBP) [21, 13, 13].

- DS: Momentum conserving Ducros et al. skew-symmetric split of the inviscid flux derivative [2].

- KGP: Kennedy-Gruber-Pirozzoli (KGP) skew-symmetric splitting of the inviscid flux derivative that is kinetic energy preserving [5, 8, 1].

- ESDS: Entropy split with Ducros et al. splitting [13].

- ESSW: Entropy split with Ducros et al. splitting but switch to regular central near discontinuities [14].

- ECLOGKP: Tadmor-type entropy conserving method using the E_L entropy function with Ranocha's kinetic energy preserving modification [9].

- DSKP: Ducros Split with kinetic energy preservation.

From our previous studies [13, 15, 14], the Tadmor-type entropy conserving methods ECLOG and ECLOGKP are the most CPU intensive methods among the nine methods. They use approximately twice the CPU time per time step than the ES, ESDS and ESSW methods. DS is the least CPU intensive. Comparison of execution times were given in previous published works.

3D shock-free compressible turbulence gas dynamics test case – 3D Taylor-Green vortex

The well-known shock-free compressible turbulence test case to evaluate the stability and accuracy for gas dynamics is the Taylor-Green vortex [19] . The 3D Euler equations of compressible gas dynamics are solved with $\gamma = 5/3$. The computational domain is a cube with sides of length 2π and with periodic boundary conditions in all three directions. The initial data are

$$\rho = 1 \quad p = 100 + ((\cos(2z)+2)(\cos(2x)+ \cos(2y)) - 2)/16$$
$$u = \sin x\cos y\cos z,\ v = -\cos x\sin y\cos z,\ w = 0.$$

The problem is solved to time 20. In our previous studies, solutions on a uniform coarse grid with 64^3 grid points were compared with a filtered DNS solution computed on a fine uniform grid with 256^3 grid points. Here, we use the same uniform coarse grid to examine the nonlinear stability and accuracy of the eight-order accurate version of the methods. The total kinetic energy of the exact solution is constant in time.

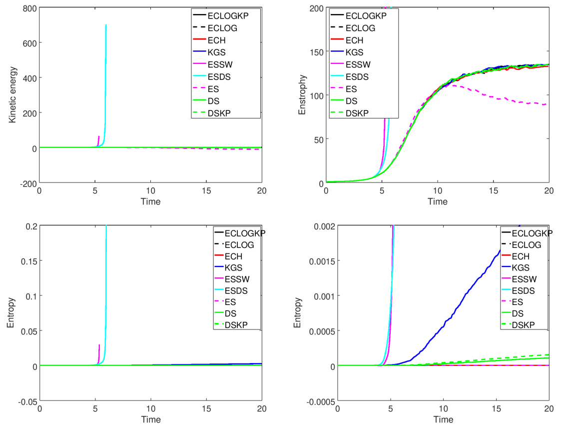

Figure 3: 3D inviscid Taylor-Green vortex using 64^3 grid points: Comparison of kinetic energy (top left), enstrophy (top right), entropy (bottom left) and entropy (closed up, bottom right) vs. time for the nine eighth-order methods using $\beta = 2$.

The present discussion of numerical results is confined to a coarse grid DNS comparison among methods. It is noted that for this Taylor-Green inviscid problem, small scales are generated that eventually cause large errors in the solution due to inadequate resolution. This occurs around $T \approx 5$. Another issue is that for very low dissipative or non-dissipative numerical methods for the simulation of turbulent flows, even with extreme grid refinement, grid convergence cannot be obtained as the original inviscid Euler equations are chaotic in nature. With sufficient but not excess numerical dissipations, one is then solving the equivalent of a Navier-Stokes equations. See Yee & Sjögreen [26] for a study. The end time is 20 instead of the standard end time 10 to observe the solution behavior twice as long using the same RK4 time discretization and CFL number 0.4. Figure 3 shows the comparison of total kinetic energy, enstrophy, and entropy vs. time for the nine eighth-order methods. It is interesting to see the behavior of doubling the time integration duration for such a coarse grid DNS computation. Method ESDS becomes unstable at around time 6, and method DSKP becomes unstable around time 7. All other schemes ran to completion. Again, the kinetic energy and entropy results show the quantity with its value at time zero subtracted, e.g., for the kinetic energy ($E_{kin}(t)$) the plotted quantity is $E_{kin}(t) - E_{kin}(0)$. The ES method starts to lose some energy at a later time. Otherwise the stable results are similar. ECLOGKP and KGS are indistinguishable, and fall on top of each other in the zoomed in figure. One surprising result is that method ECHKP (labeled ECH in the plots) is expected to preserve kinetic energy in the same manner but does not. The other stable methods are a little off, but it is only visible in the closeup. Methods ES and ECHKP fall on top of each other, as we would expect, since these two schemes conserve the entropy in a discretized sense. Method ECLOGKP is also on top of ES and ECHKP, making it hard to visualize the differences in the results.

Not shown here, studies show that the logarithmic entropy function conserved Harten's entropy almost perfectly. Methods ECLOGKP and ECLOG conserve entropy as illustrated in the figure where their solutions are on top of each other. Overall, ECLOGKP, ECLOG, ECHKP, KGS, and DS are very similar. One has to zoom in very much on the plots to see any differences for this test case. However, differences might be larger for other flow problems. As can be seen, for this test case, method ES behaves somewhat different. DSKP and ESDS are not performing well. It is noted again that results by ES and ESDS are highly dependent on the entropy splitting parameter β (which is related to the parameter α in E_H). Only results by $\beta = 2$ are shown based on the study in [13].

Harten's entropy was used for all schemes except ECLOG and ECLOGKP where we used the log-entropy.

5 Concluding Remark

It is our assessment that a high order nonlinear filter method with structural-preserving properties is a viable approach to help improve the predictability and reliability of the onset of shock-free turbulence and turbulence with shocklets. For turbulence with shocks, there is an even larger gain both in accuracy and CPU time of the nonlinear filter schemes over their standard variants of ENO/WENO counterparts or their hybrid counterparts (by switching between non-dissipative high order methods and high order shock-capturing methods).

6 *

References

[1] G. Coppola, F., Capuano, S. Pirozzoli and L. de Luca *Numerically Stable Formulations of Convective Terms for Turbulent Compressible Flows*, J. Comput. Phys .. 2019, DOI: 10.1016/j.jcp.2019.01.007.

[2] F. Ducros, F. Laporte, T. Soulères, V. Guinot, P. Moinat, and B. Caruelle, *High-order Fluxes for Conservative Skew-Symmetric-like Schemes in Structured Meshes: Application to Compressible Flows*, *J. Comp. Phys.*, **161** 114–139 (2000).

[3] A. Harten *On the Symmetric Form of Systems for Conservation Laws with Entropy*, J. Comput Phys. 49, 151 (1983).

[4] A. Hadjadj, H.C. Yee and B. Sjogreen, LES of Temporally Evolving Mixing Layers by an

Eighth-Order Filter Scheme, AIAA-ASM meeting, Jan. 9-12, 2012 Nashville, TN; *International J. Num. Meth. Fluids*, 70:1405-1427, 2012.

[5] C.A. Kennedy and A. Gruber, *Reduced Aliasing Formulations of the Convective Terms Within the Navier-Stokes Equations*, J. Comput. Phys .. 227 1676-1700 (2008).

[6] Dmitry V. Kotov, H.C. Yee, Marco Panesi, and Dinesh K. Prabhu, *Computational Challenges for Simulations Related to the NASA Electric Arc Shock Tube (EAST) Experiments*; J. Comput. Phys., **269** 215-233 (2014).

[7] D.V. Kotov, H.C. Yee, A.A. Wray, B. Sjögreen, and A.G. Kritsuk, *Numerical Dissipation Control in High Order Shock-Capturing Schemes for LES of Low Speed Flows*, *J. Comput. Phys.*, **307** 189–202 (2016).

[8] S. Pirozzoli, *Generalized Conservative Approximations of Split Convective Derivative Operators*, J. Comput. Phys., 219, 7180-90 (2010).

[9] H. Ranocha *Entropy Conserving and Kinetic Energy Preserving Numerical Methods for the Euler Equations Using Summation-by-Parts Operators*, Proceedings of the ICOSAHOM:-2018, Imperial College, London, UK, July 9-13, 2018.

[10] B. Sjögreen and H. C. Yee, *Multiresolution Wavelet Based Adaptive Numerical Dissipation Control for Shock-Turbulence Computation*, *J. Scient. Computing*, **2** 211–255 (2004).

[11] B. Sjögreen and H.C. Yee, *High Order Entropy Conserving Central Schemes for Wide Ranges of Compressible Gas Dynamics and MHD Flows*, J. Comput. Phys., **364**, 153-185 (2018).

[12] B. Sjögreen and H.C. Yee, *On High Order Entropy Conservative Numerical Flux for Multiscale Gas Dynamics and MHD Simulations*, Proceeding of ICOSAHOM 2016, Lecture Notes in Computational Science and Engineering, vol. 119, Springer (2017).

[13] B. Sjögreen, and H.C. Yee, *Entropy Stable Method for the Euler Equations Revisited: Central Differencing via Entropy Splitting and SBP*, J. Scientific Computing, 81:1359-1385 (2019), https://doi.org/10.1007/s10915-019-01013-1.

[14] B. Sjögreen and H.C. Yee, *Construction of Conservative Numerical Fluxes for the Entropy Split Method*, Comm. Applied Mathematics and Computation (CAMC), 2021.

[15] B. Sjögreen, H.C. Yee, D. V. Kotov and A. G. Kritsuk, *Skew-Symmetric Splitting for Multiscale Gas Dynamics and MHD Turbulence Flows*, J. Scientific Computing, 83:1-43, (2020)

[16] B. Sjögreen and H.C. Yee, *High Order Compact Central Spatial Discretization Under the Framework of Entropy Split Methods*, Proceedings of the ICOSAHOM21, July 12-16, 2021.

[17] E. Tadmor *Entropy Stability Theory for Difference Approximations of Nonlinear Conservation Laws and Related Time-Dependent Problems* Acta Numerica 12, 451-512 (2003).

[18] E. Tadmor *Entropy Stability Theory for Difference Approximations of Nonlinear Conservation Laws and Related Time-Dependent Problems*, *Acta Numerica*, **12**, pp. 451–512 (2003).

[19] G. Taylor and A. Green, *Mechanism of the Production of Small Eddies from Large Ones*, Proc. R. Soc. Lond. A 158, 499-521 (1937).

[20] H. C. Yee, N. D. Sandham, and M. J. Djomehri, *Low Dissipative High Order Shock-Capturing Methods Using Characteristic-Based Filters*, J. Comput. Phys., **150** 199–238 (1999).

[21] H. C. Yee, Marcel Vinokur, and M. J. Djomehri, *Entropy Splitting and Numerical Dissipation* J. Comput. Phys., **162** 33–81 (2000).

[22] H.C. Yee, *Building Blocks for Reliable Complex Nonlinear Numerical Simulations* **Turbulent Flow Computation**, Kluwer Academic, (2002).

[23] H.C. Yee and B. Sjögreen, *Efficient Low Dissipative High Order Schemes for Multiscale MHD Flows, II: Minimization of div(B) Numerical Error*, *J. Sci. Comp.*, **29** 910–934 (2006).

[24] W. Wang, C.-W. Shu, H.C. Yee and S. Sjögreen, *High Order Finite Difference Methods with Subcell Resolution for Advection Wquations with Stiff Source Terms*, J. Comput. Phys., **231** 190–214 (2012).

[25] H.C. Yee and B. Sjögreen, Development of Low Dissipative High Order Filter Schemes for Multiscale Navier-Stokes/MHD Systems, *J. Comput. Phys.*,**225** 910–934 (2007).

[26] H.C. Yee and B. Sjögreen, *Simulation of Richtmyer-Meshkov Instability by Sixth-Order Filter Methods*, Proceedings of the 17th International Shock Interaction Symposium; also *Shock Waves Journal*, **17** 185–193, (2007).

[27] H.C. Yee and B. Sjögreen, *High Order Filter Methods for Wide Range of Compressible Flow Speeds*, Proceedings of ICOSAHOM 09 (International Conference on Spectral and High Order Methods). June 22–26, 2009, Trondheim, Norway.

[28] H.C. Yee, D. V. Kotov, Wei Wang and Chi-Wang Shu, Spurious behavior of shock-capturing methods by the fractional step approach: Problems containing stiff source terms and discontinuities, J. Comput. Phys., **241** 266-291 (2013).

[29] H.C. Yee and B. Sjögreen, *On Entropy Conservation and Kinetic Energy Preservation Methods* Proceedings of the ICOSAHOM-2019, July 1-5, 2019, Paris, France.

[30] H.C. Yee and B. Sjögreen, *Comparative Study on a Variety of Structure-Preserving High Order Spatial Discretizations with the Entropy Split Methods for MHD*. Proceedings of the ICOSAHOM21, July 12-16, 2021.

[31] H.C. Yee and B. Sjögreen, *Recent Advancement of Entropy Split Methods for Compressible Gas Dynamics and MHD*, J. Appl. Math. Comput., A special issue in the Journal of Applied Mathematics and Computation (ACM) on Hyperbolic PDE in computational physics: Advanced Mathematical Models and Structure-Preserving Numerics, 2022.